Imaging through a weakly scattering medium by spectral-domain optical coherence microscopy with a digital phase conjugation

Nakatani, Noriyuki
Takeuchi, Shota
Harukaze, Keisuke
Quan, Xiangyu
Matoba, Osamu

(Citation)
Optics Continuum,2(1):155-163

(Issue Date)
2023-01-15

(Resource Type)
journal article

(Version)
Version of Record

(URL)
https://hdl.handle.net/20.500.14094/0100483200

Research Article Vol. 2, No. 1 / 15 Jan 2023 / Optics Continuum 155
OPTICS CONTINUUM

Imaging through a weakly scattering medium by spectral-domain optical coherence microscopy with a digital phase conjugation

NORIYUKI NAKATANI,[1] SHOTA TAKEUCHI,[1] KEISUKE HARUKAZE,[1] XIANGYU QUAN,[1,2] AND OSAMU MATOBA[1,2,*]

[1]*Graduate School of System Informatics, Kobe University, Rokkodai 1-1, Nada, Kobe 657-8501, Japan*
[2]*Center of Optical Scattering Image Science, Kobe University, Rokkodai 1-1, Nada, Kobe 657-8501, Japan*
[*]*matoba@kobe-u.ac.jp*

Abstract: A spectral-domain optical coherence microscope (SD-OCM) embedded by a digital phase conjugation is presented for high-resolution imaging of objects behind a weakly scattering medium. For high-resolution SD-OCM, keeping a narrow focusing spot even in a scattering medium is important. To compensate for the degradation of the focused spot due to the scattering, digital phase conjugation with a low-coherent light is introduced by measuring the distorted wavefront of coherent light and making wavelength conversion due to the difference between the coherent and low-coherent light beams. Experiments using a weakly scattering sheet with a scattering angle of 30 degrees showed us to improve the focused spot property and enhance the reflected intensity signal. We also demonstrate the feasibility of the system for the imaging of objects with periodic reflectance structures of 10 μm width.

1. Introduction

In recent years, the field of imaging through scattering or turbid medium has undergone significant development. In order to extract object information through the scattering medium, several techniques including the combination of autocorrelation operations and phase recovery [1], transmission matrix or nonnegative matrix factorization [2,3], and machine learning [4], have been reported. A speckle pattern is generated by scattering or random phase modulation. The speckle phenomenon has been used in image encryption such as double random phase encryption [5]. The decryption is done by compensating for the phase modulation by a random phase mask and restoring the original image [5–8]. The development of phase-mode spatial light modulators (SLMs) has made it possible to compensate for phase distortion caused by multimode fibers or turbid media using digital phase conjugation techniques [9–12]. It is also possible to compensate for aberrations generated by optical elements in digital holography [13].

Imaging in a scattering medium is an attractive research field that can be applied to biomedical imaging for noninvasive observation of absorption or fluorescence distribution in biological tissues. In two-photon excitation microscopy, phase compensation is used to extend the depth of observation [14]. Optical coherence tomography (OCT) is one of the powerful tools to obtain three-dimensional reflectance images inside biological tissues [15,16]. OCT with microscopic applications is called optical coherence microscopy (OCM) [17–19]. There are two major problems in overcoming scattering phenomena in OCM. One problem is that the focusing property of the light inside the scattering medium is degraded. Broadening the focused spot degrades the spatial resolution of the OCM imaging and reduces the reflected signal. The second problem is to remove the scattered light and extract the ballistic and snake light for depth measurement. For the first problem, a method using a long wavelength with a small scattering coefficient is effective [19]. For the second problem, there is a method to use coherence gating or short-pulsed light. High-resolution OCT techniques have been presented for fundus imaging

#480436 https://doi.org/10.1364/OPTCON.480436
Journal © 2023 Received 9 Nov 2022; revised 12 Dec 2022; accepted 12 Dec 2022; published 3 Jan 2023

OPTICS CONTINUUM

using adaptive optics. One is composed of a Shack-Hartmann wavefront sensor to detect the wavefront distortion by the eyeball and a deformable mirror to compensate for the wavefront distortion [20] and the combination of a pyramid wavefront sensor and deformable mirror [21]. High-resolution imaging of the retina by scanning the focal point is also being investigated using a wavefront sensor and a spatial light modulator for wavefront distortion caused by the eyeball [22]. Many researches focus on retina imaging and deal with the correction of aberrations mainly expanded by the Zernike polynomial. Here, when we deal with speckles due to scattering, wavefront measurement requires a higher spatial resolution. In addition, a phase-modulated spatial light modulator with a large number of pixels is required to compensate for the speckles.

In this paper, we deal to overcome these two problems by proposing a spectral-domain OCM (SD-OCM) system that uses digital phase conjugation to focus light through a scattering medium to improve spatial resolution and reflected signal. The phase distortion due to the scattering medium is measured by interferometry using a laser beam, and the super luminescent diode (SLD) light used as the probe light for SD-OCM is modulated to obtain a focused spot after passing through the scattering medium. Since the wavelengths of the laser light and the SLD light are different, a correction phase change is calculated according to the wavelength ratio. Experiments with a weakly scattering medium show the improvement of the performance of the focused spot and OCM signal operated at 1 Hz, and show the two-dimensional imaging results. These experimental results demonstrate the effectiveness of the proposed method.

2. SD-OCM system with digital phase conjugate mirror

Figure 1 shows the SD-OCM system with a digital phase conjugate mirror. This system consists of an interferometer to measure the wavefront of the scattered light after a laser light beam passes through a scattering medium, and an SD-OCM system with a digital phase conjugate mirror using a phase-modulated spatial light modulator. The SD-OCM system uses low coherence light to achieve a narrow depth range that is a coherence gate. It is not good for an optical interferometer due to low temporal and spatial coherence. Therefore, a laser beam is required for wavefront measurement caused by the scattering medium. In general, the wavelength of the laser beam does not coincide with the central wavelength of the low-coherence light, so it is necessary to perform wavelength conversion from the wavefront measurement result using the laser light to the wavefront modulation of the low-coherence light.

First, we describe the interferometer used to measure the wavefront of the scattered light in Fig. 1(a). A He-Ne laser beam, Melles griot 05-LHP-111, which is a coherent light source, is split into two parts by a beam splitter. The object light is focused by an objective lens, Olympus ULWD MSPlan 20, with NA 0.4 and a focal length of 9 mm, and then passes through the scattering medium. The modulated object light interferes with the reference light that does not pass through the scattering medium, and the interference pattern is captured by an image sensor (CCD1). An off-axis interference fringe is obtained, and the amplitude and phase distributions are obtained by the fringe analysis based on the Fourier transform. Here, the phase distribution is used for generating a phase conjugate wave in the SLD.

Next, we present an SD-OCM system with a digital phase conjugate mirror using a low-coherence light source, SLD Superlum S785-B-I-15, at the central wavelength of 785 nm and wavelength width of 18 nm. The SLD light is phase-modulated by a phase-mode spatial light modulator, LCOS-SLM (liquid crystal on silicon spatial light modulator), and then the phase distribution is corrected by passing through a scattering medium. The LCOS-SLM, Hamamatsu X10468-01, has a pixel pitch of 20 µm and number of pixels of 600 × 800, while CCD 1, FLIR BFLY-U3-23S6, has a pixel spacing of 5.86 µm and a pixel count of 1200 × 1920. Therefore, pixel pitch and number of pixels between CCD and LCOS-SLM are different. So, we need to transform a phase distribution to be displayed on the LCOS-SLM from the phase distribution obtained by CCD1. To confirm that the phase correction is effectively worked, the following two

OPTICS CONTINUUM

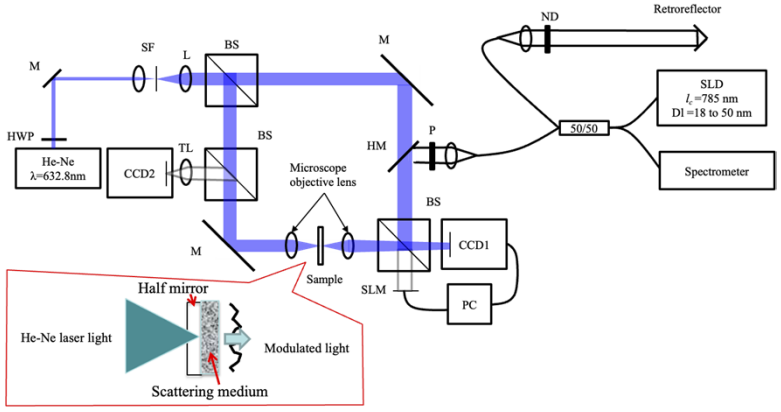

(a)

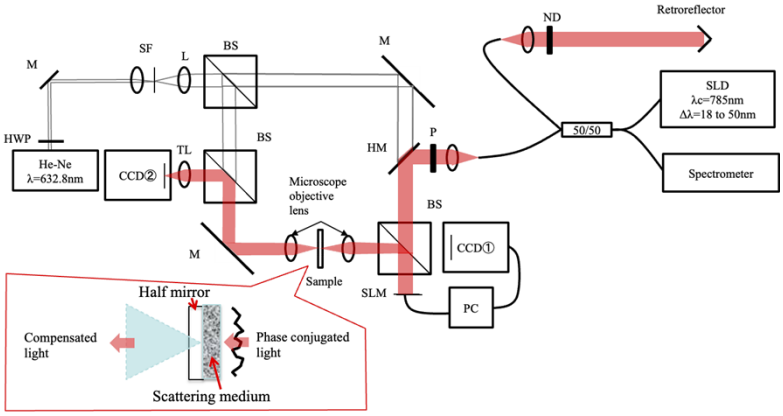

(b)

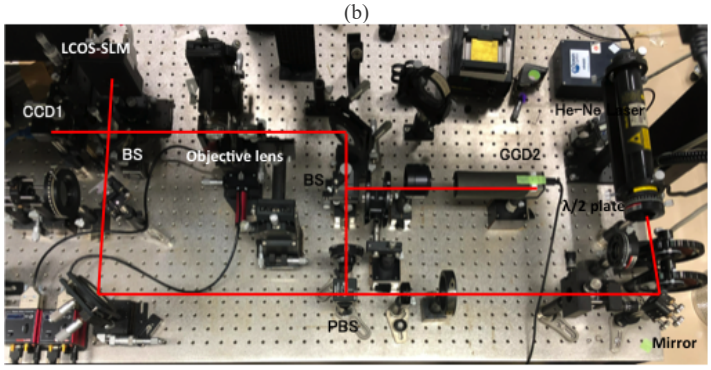

(c)

Fig. 1. Optical setup of SD-OCT with digital phase conjugation for image quality improvement in weakly scattered medium. (a) Measurement of scattered light by an interferometer using a He-Ne laser, (b) SD-OCT using an SLD, and (c) the photograph. HWP, half-wave plate; M, mirror; SF, spatial filter; L, lens; BS, beam splitter; HM, half mirror; P, polarizer; TL, tube lens; ND, neutral density filter; SLM, spatial light modulator.

OPTICS CONTINUUM

issues are checked. The phase-correction of SLD light passing through the scatteringmedium is checked by obtaining the focused spot of light in an image sensor (CCD2), Thorlabs DCU224 with 1280 × 1024 pixels and pixel pitch of 4.65 μm. Another check is the increase of OCM signal. The SLD light is interfered by an optical-fiber based interferometer with two lights reflected from an object beyond the scattering medium and a reference mirror, respectively. From the obtained interference spectra by a spectrometer, Ocean Optics, HR4000 (699 nm-889 nm) with 3,648 pixels, a reflectance profile along the depth direction is obtained by Fourier transform.

As described above, the wavelength of the He-Ne laser light at 632.8 nm and the central wavelength of the SLD at 785 nm are different, so it is necessary to create a phase distribution with the phase amount adjusted to match the wavelength ratio. Figure 2 shows the process required to generate the digital phase conjugate wave. Here, there is no scattering medium and a half mirror without a scattering medium is located. As shown in Fig. 1, a He-Ne laser beam is focused by an objective lens and then an output beam after propagation by a scattering medium is imaged on CCD1 by using a single lens. When there is no scattering medium, a slightly defocused beam due to the propagation through the sample thickness is observed. Therefore, a spherical phase distribution is observed as shown in the phase distribution on the left in Fig. 2. This spherical phase distribution is unwrapped from the phase distribution $P_1(x,y)$ measured with a He-Ne laser beam. In this study, the Goldstein method [23] was used to eliminate the phase jump when the phase distribution is distorted by a scattering medium. After the phase unwrapping, the phase amount is changed according to the wavelength ratio between the He-Ne laser and the SLD. Then, the phase is wrapped by the wavelength of SLD. After the wavelength conversion from He-Ne laser to SLD, the phase distribution to be displayed on the LCOS-SLM is obtained as shown in the phase map on the right in Fig. 2. Here, we assume that the phase distribution is caused by a scattering medium, not by the object sample. The difference between phase distribution and an ideal spherical wave is the wave difference caused by the scattering medium. This system can update the phase distribution as digital phase conjugation at 1 Hz.

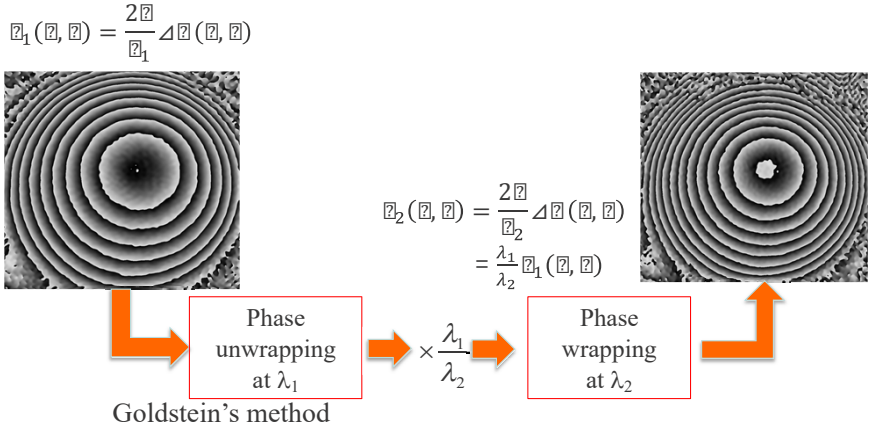

Fig. 2. Process of obtaining phase conjugate distribution from the measurement of the optical interferometer. Here, in the experiment, there is no scattering medium and then spherical wavefront obtained at defocused position can be seen. The difference between phase distribution and an ideal spherical wave is the wave difference caused by the scattering medium.

3. Experimental results

Two experiments were conducted to verify the operation of this system. First, a half-mirror as a transmitted object attached to a scattering sheet was used to show the improvement of the focused

OPTICS CONTINUUM

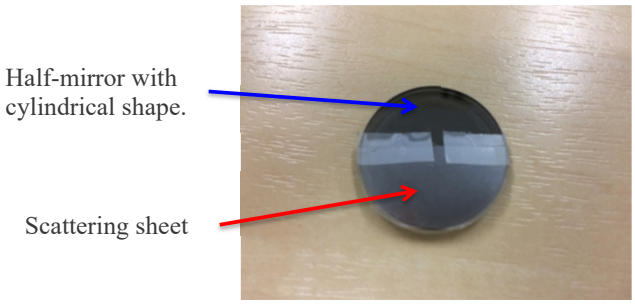

Fig. 3. The measured object. A scattering sheet is attached to the lower half of the surface of a half-mirror with cylindrical shape.

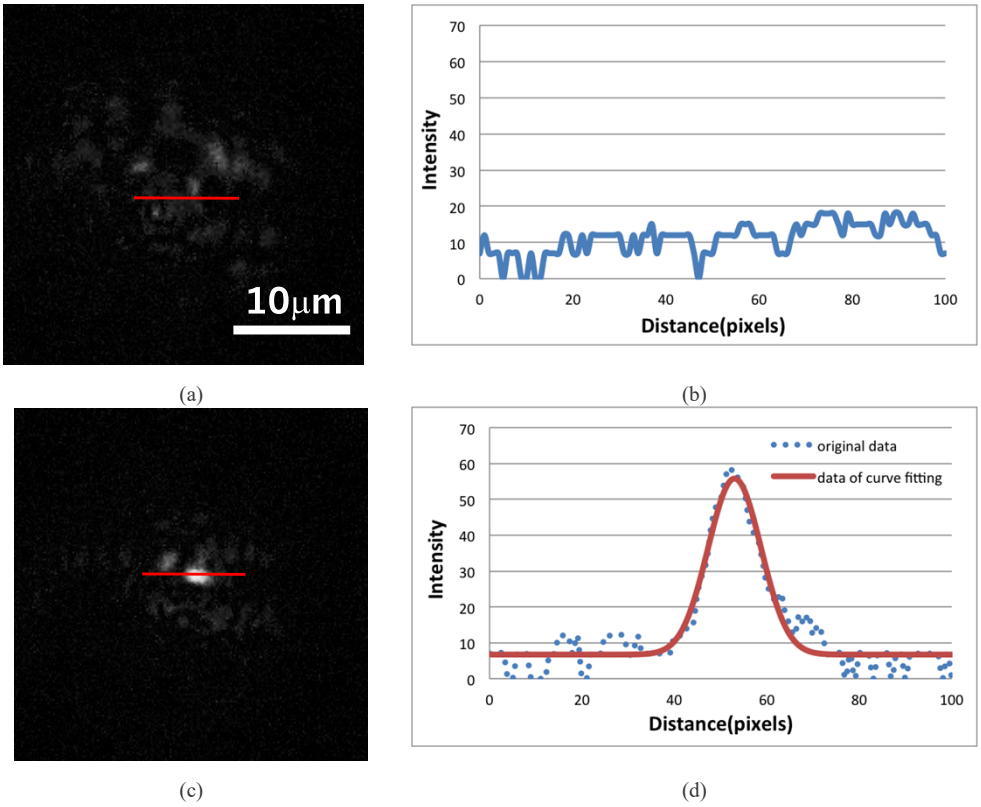

Fig. 4. Spot profiles of SLD light observed at CCD2. (a) and (b) intensity image and its profile of SLD light without digital phase conjugation, (c) and (d) intensity image and its profile of SLD light with digital phase conjugation.

spot shape and the enhancement of the OCM signal by digital phase conjugation. Next, an object with a spatially structured periodic reflectance was used for scan imaging.

First, we show the improvement of the focused spot shape and the enhancement of the OCT signal by digital phase conjugate wave generation. A scattering sheet at a scattering angle of 30 degrees and a thickness of 0.1 mm. The scattering sheet is attached to the lower half of the surface of a half-mirror with a cylindrical shape as shown in Fig. 3. Figure 4 shows the change of the focused spot of the SLD with and without the digital phase conjugation. Figures 4(b) and

OPTICS CONTINUUM

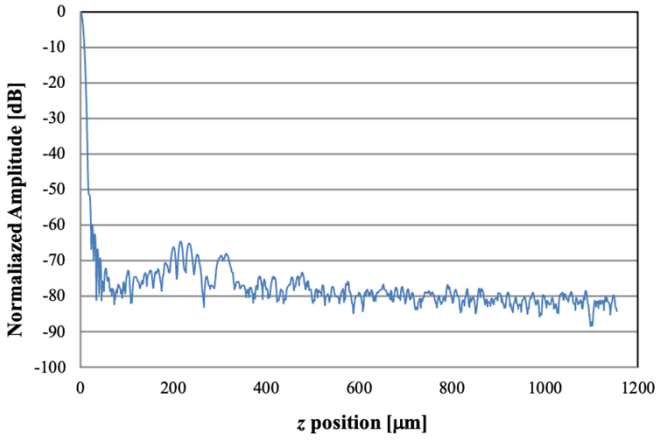

(a)

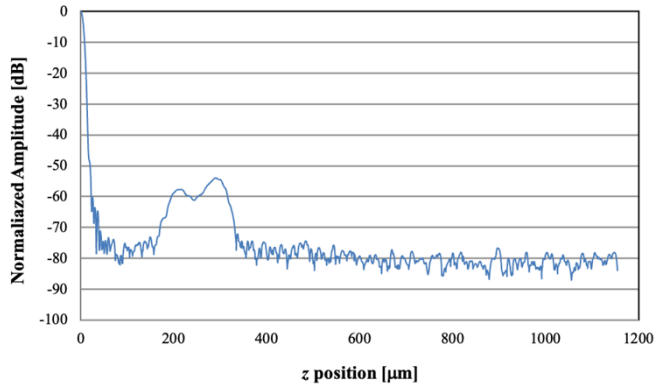

(b)

Fig. 5. Improvement of OCM signal of the object of Fig. 4. Reflected signal along the depth position (a) without and (b) with digital phase conjugation.

(d) show the cross-sectional distributions of Figs. 4(a) and (c), respectively. Without the digital phase conjugation, the wavefront is modulated by the scattering sheet and the focused spot cannot be seen in Fig. 4(a). We can see the distorted intensity pattern such as the speckle in Fig. 4(a) and then it is clearly understood that the Shack-Hartmann wavefront sensor cannot be applied. The phase modulation by the scattering sheet is canceled by the digital phase conjugate wave and the focused spot was seen as in Fig. 4(c). The spot diameter ($1/e^2$ full-width) is 3.18 μm. The beam width at the diffraction limit is 1.20 μm, which is 2.79 times wider than the diffraction limit. A video file of the focused spot without and with digital phase conjugation is shown in Visualization 1. Figure 5 shows the results of the OCM reflection intensity measurements as a function of the depth. There are two peaks in Fig. 5(b) due to the front and rear surface reflection of the scattering medium. The rear surface is attached to the half mirror and then the second peak is relatively higher than the first one. The peak values in Figs. 5(a) and (b) are -75.0 dB and -55.0 dB, respectively. This result indicates that the peak difference between the two graphs is 20 dB, which means that the reflected light intensity was improved by a factor of about 17.84. A video file of the OCM profile with and without phase correction by the digital phase conjugate

OPTICS CONTINUUM

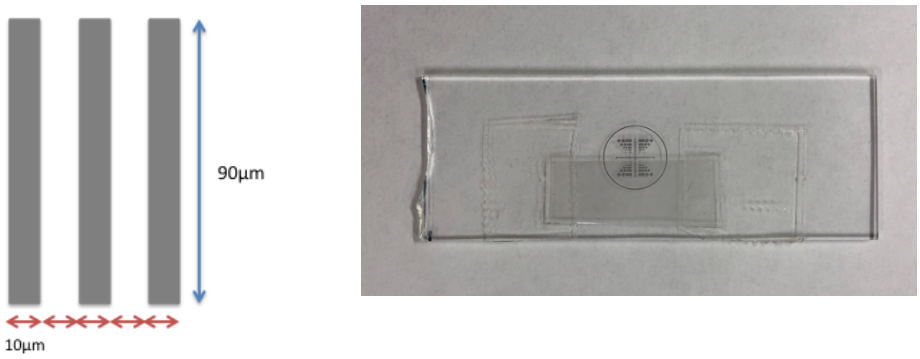

(a) (b)

Fig. 6. The two-dimensional periodic object with a scattering sheet. (a) Measured region of the two-dimensional periodic object and (b) the photography after attaching the scattering sheet. The scattering sheet is attached to the lower half of the surface of the two-dimensional periodic object.

mirror is shown in Visualization 2. You can see easily the focusing spot when the digital phase conjugate mirror turns on.

The two-dimensional periodic object as shown in Fig. 6 was then measured by the proposed system. The periodic object has a different reflectance in every 10 μm steps along the x-axis. The object is scanned horizontally at a step of 3.3 μm to obtain 19 points (along the x-axis) and vertically at a step of 10 μm by movable stages to obtain 11 points (along the y-axis). The movable stages are controlled by a computer. 10 measurements were taken at each point and the results of the average reflection intensity are shown in Figs. 7(a)–(b). Figures 7(a) and (b) show the reflectance distributions without and with digital phase conjugation, respectively. We evaluate the improvement of the reflectance with and without digital phase conjugation. The reflected signals in the object region and outside the region of the object by using digital phase conjugation are -31.77 dB and -40.16 dB, respectively. The reflected signals in the object region and outside the region of the object without digital phase conjugation are -43.55 dB and -47.38 dB, respectively. The differences between the object and the outside region are 8.39 dB and 3.83 dB. A comparison of Figs. 7(a) and (b) shows that the phase conjugate wave generation enabled clearer imaging

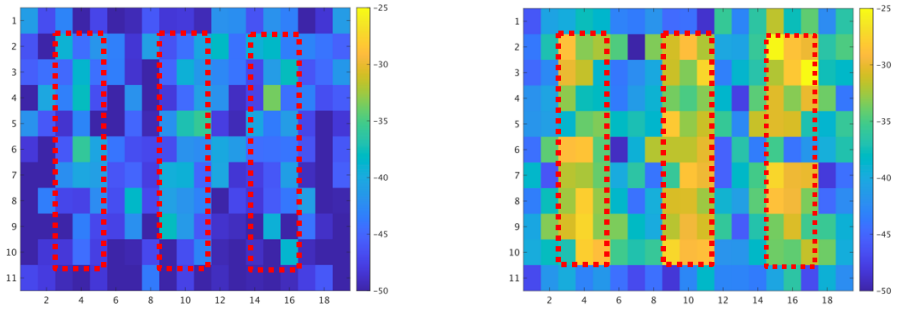

(a) (b)

Fig. 7. Reflectance images by scanning the focused point (a) without and (b) with digital phase conjugation. Red dashed regions indicate the high-reflectance region.

OPTICS CONTINUUM

of the three-line structure. In Fig. 7(b), a part of the reflectance is low which can be attributed to temporal atmospheric fluctuations. To counteract this problem, the optical system can be enclosed so as to reduce the effect of atmospheric turbulence and disturbance.

4. Conclusion

In this paper, we have presented an SD-OCM system using a digital phase conjugate mirror for achieving high-resolution imaging of objects behind a weakly scattering medium. An optical interferometer is introduced to measure the wavefront degradation caused by the scattering medium, and phase conjugate waves are generated for the low-coherence light after wavelength conversion. Experiments with a scattering sheet produced a focused spot 2.79 times larger than the beam waist and a reflected intensity signal about 17.84 times larger. It was also demonstrated that imaging of an object with a 10 µm wide periodic reflectance structure is possible. The operating speed of the system is 1 Hz.

Funding. Japan Society for the Promotion of Science (JSPS) KAKENHI Grant Number (20H05886).

Disclosures. The authors declare that there are no conflicts of interest related to this article.

Data availability. Data underlying the results presented in this paper are not publicly available at this time but may be obtained from the authors upon reasonable requests

References

1. J. Bertolotti, E. G. van Putten, C. Blum, A. Lagendijk, W. L. Vos, and A. P. Mosk, "Non-invasive imaging through opaque scattering layers," Nature **491**(7423), 232–234 (2012).
2. S. M. Popoff, G. Lerosey, R. Carminati, M. Fink, A. C. Boccara, and S. Gigan, "Measuring the transmission matrix in optics: an approach to the study and control of light propagation in disordered media," Phys. Rev. Lett. **104**(10), 100601 (2010).
3. A. Boniface, J. Dong, and S. Gigan, "Non-invasive focusing and imaging in scattering media with a fluorescence-based transmission matrix," Nat. Commun. **11**(1), 6154 (2020).
4. R. Horisaki, R. Takagi, and J. Tanida, "Learning-based imaging through scattering media," Opt. Express **24**(13), 13738–13743 (2016).
5. P. Refregier and B. Javidi, "Optical image encryption based on input plane encoding and Fourier plane random encoding," Opt. Lett. **20**(7), 767–769 (1995).
6. O. Matoba and B. Javidi, "Encrypted optical memory system using three-dimensional keys in the Fresnel domain," Opt. Lett. **24**(11), 762–764 (1999).
7. O. Matoba, T. Nomura, E. Perez-Cabre, M. Millan, and B. Javidi, "Optical techniques for information security," Proc. IEEE **97**(6), 1128–1148 (2009).
8. B. Javidi and T. Nomura, "Securing information by use of digital holography," Opt. Lett. **25**(1), 28–30 (2000).
9. I. N. Papadopoulos, S. Farahi, C. Moser, and D. Psaltis, "Focusing and scanning light through a multimode optical fiber using digital phase conjugation," Opt. Express **20**(10), 10583–10590 (2012).
10. T. R. Hillman, T. Yamauchi, W. Choi, R. R. Dasari, M. S. Feld, Y. K. Park, and Z. Yaqoob, "Digital optical phase conjugation for delivering two-dimensional images through turbid media," Sci. Rep. **3**(1), 1909 (2013).
11. Y. W. Yu, C. C. Sun, W. H. Chen, S. Y. Chen, Z. S. Hou, C. C. Lin, and P. K. Hsieh, "Continuous amplified digital optical phase conjugator for focusing through thick, heavy scattering medium," OSA Continuum **2**(3), 703–714 (2019).
12. Y. W. Yu, S. Y. Chen, C. C. Lin, and C. C. Sun, "Inverse focusing inside turbid media by creating an opposite virtual objective," Sci. Rep. **6**(1), 29452 (2016).
13. L. Miao, K. Nitta, O. Matoba, and Y. Awatsuji, "Parallel phase-shifting digital holography with adaptive function using phase-mode spatial light modulator," Appl. Opt. **51**(14), 2633–2637 (2012).
14. A. Tanabe, T. Hibi, S. Ipponjima, K. Matsumoto, M. Yokoyama, M. Kurihara, N. Hashimoto, and T. Nemoto, "Correcting spherical aberrations in a biospecimen using a transmissive liquid crystal device in two-photon excitation laser scanning microscopy," J. Biomed. Opt. **20**(10), 101204 (2015).
15. D. Huang, E. A. Swanson, C. P. Lin, J. S. Schuman, W. G. Stinson, W. Chang, M. R. Hee, T. Flotte, K. Gregory, C. A. Puliafito, and J. G. Fujimoto, "Optical Coherence Tomography," Science **254**(5035), 1178–1181 (1991).
16. J. G. Fujimoto, "Optical coherence tomography for ultrahigh resolution in vivo imaging," Nat. Biotechnol. **21**(11), 1361–1367 (2003).
17. J. A. Izatt, M. R. Hee, and G. M. Owen, "Optical coherence microscopy in scattering media," Opt. Lett. **19**(8), 590–592 (1994).
18. J. M. Schmitt, S. L. Lee, and K. M. Yung, "An optical coherence microscope with enhanced resolving power in thick tissue," Opt. Commun. **142**(4-6), 203–207 (1997).

OPTICS CONTINUUM

19. M. Yamanaka, T. Teranishi, H. Kawagoe, and N. Nishizawa, "Optical coherence microscopy in 1700 nm spectral band for high-resolution label-free deep-tissue imaging," Sci. Rep. **6**(1), 31715 (2016).
20. B. Hermann, E. J. Fernandez, A. Unterhuber, H. Sattmann, A. F. Fercher, W. Drexler, P. M. Prieto, and P. Artal, "Adaptive-optics ultrahigh-resolution optical coherence tomography," Opt. Lett. **29**(18), 2142–2144 (2004).
21. E. Brunner, J. Shatokhina, M. F. Shirazi, W. Drexler, R. Leitgeb, A. Pollreisz, C. K. Hitzenberger, R. Ramlau, and M. Pircher, "Retinal adaptive optics imaging with a pyramid wavefront sensor," Biomed. Opt. Express **12**(10), 5969–5990 (2021).
22. K. Takayama, S. Ooto, M. Hangai, N. Arakawa, S. Oshima, N. Shibata, M. Hanebuchi, T. Inoue, and N. Yoshimura, "High-resolution imaging of the retinal nerve fiber layer in normal eyes using adaptive optics scanning laser ophthalmoscopy," PLoS One **7**(3), e33158 (2012).
23. R. Goldstein, H. Zebker, and C. Werner, "Satellite radar interferometry: Two-dimensional phase unwrapping," Radio Sci. **23**(4), 713–720 (1988).